Geothermics 57 (2015) 205–212

Contents lists available at ScienceDirect

Geothermics

journal homepage: www.elsevier.com/locate/geothermics

Thermal investigation of in-series vertical ground heat exchangers for industrial waste heat storage

Ping Cui[a,b,*], Nairen Diao[b], Chengmiao Gao[b], Zhaohong Fang[b]

[a] Key Laboratory of Renewable Energy Utilization Technologies in Buildings, Ministry of Education, Jinan 250101, China
[b] Shandong Key Laboratory of Building Energy-saving Technique, School of Thermal Engineering, Shandong Jianzhu University, 250101, China

ARTICLE INFO

Article history:
Received 7 January 2015
Received in revised form 30 May 2015
Accepted 4 June 2015
Available online 24 July 2015

Keywords:
Multistage-series circuits
Seasonal thermal energy storage
Utilization of industrial waste heat
Ground heat exchanger

ABSTRACT

This paper presents a novel ground heat exchanger configuration with vertical boreholes connected in series to be used for the seasonal thermal storage of industrial high-temperature condensation heat. The transient simulation model of multistage-series circuits is developed and the simplex method is employed to solve the outlet/inlet temperatures and the heat transfer rate fraction of each circuit. A simplified steady-flux model is also proposed to design a large-scale seasonal heat storage system. Finally, the effects of some critical parameters on the thermal performance of the GHE with multistage-series circuits are investigated. The results show that both optimum borehole spacing and the higher thermal properties of the ground can improve the thermal efficiency of the storage system and reduce the capital cost accordingly.

1. Introduction

The installed capacity of geothermal heat pump (GHP) systems, which use the shallow geothermal energy as a heat source/sink to provide space heating and cooling, is continuously growing worldwide (Spitler, 2005; Self et al., 2013). Among various GHP systems, the GHP with vertical boreholes (i.e. ground-coupled heat pump) has attracted the greatest interest in research field and practical engineering as well, owing to its advantages of less land area requirement and the relatively stable ground temperature. However, the wide application of the ground-coupled heat pump (GCHP) technology is hindered by the imbalance of full-year cumulative heating and cooling loads in severe cold or hot areas. For heating-dominated buildings, the amounts of heat rejected to the underground in summer cannot balance the heat extracted from the ground in winter. Especially for large-scale systems with a long-term operation, the unbalanced seasonal cooling load in the underground may cause an irreversible drop of ground temperature and correspondingly a lower temperature of circulating fluid entering the heat pump (Bayer et al., 2014). As a result, the imbalance of annual ground thermal loads will significantly degrade the system operation performance, even causing the system to collapse during the coldest time of winter.

The effective approach to eliminate the cooling load accumulation in the ground is to recharge additional heat into the ground through some mechanisms during non-heating seasons, such as the solar thermal energy and the industrial waste heat. During the last decade, many studies have been carried out to investigate the performance of the seasonal storage of solar heat energy (Pinel et al., 2011; Zhu et al., 2014). Trillat-Berdal et al. (2006) conducted an experimental study of a GCHP combined with thermal solar collectors. Solar heat was preferentially used to heat domestic hot water, while the excess of solar energy was injected into the ground. Their research results show that the system can balance the ground thermal loads, increasing the operating time of solar collectors. Some researchers focused on the studies in terms of the operation performance of the hybrid GCHP system with solar collectors through experiments or simulation (Yang et al., 2006; Ozgener and Hepbasli, 2007; Chen et al., 2011; Farzin et al., 2013). The design optimization of the complex GCHP system with solar collectors and the relative optimal control strategies have been reported by some related references (Kjellsson et al., 2010; Bayer et al., 2014; Si et al., 2014). However, only few studies have been carried out to investigate the thermal performance of the seasonal storage of industrial waste heat in the case of a designed heat and power cogeneration unit (Reuss et al., 1997). In this case study, about 418 MWh/a heat was charged into the ground at a temperature of 80 °C and about 266 MWh/a heat can be extracted from the ground and delivered

* Corresponding author at: School of Thermal Engineering, Shandong Jianzhu University, 250101, China. Tel.: +86 53166368216.
E-mail address: nature_cui@126.com (P. Cui).

http://dx.doi.org/10.1016/j.geothermics.2015.06.003
0375-6505/

Nomenclature

a	thermal diffusivity (m^2/s)
A or B	borehole spacing (m)
c	heat capacity (J/(kg K))
H	borehole depth (m)
k_g	ground thermal conductivity (W/(m K))
M	mass flow rate (kg/s)
Q	heat transfer rate (W)
q_l	heat flow per unit length of borehole (W/m)
R	thermal resistance (m K/W)
r_b	borehole radius (m)
t	temperature (°C)

Subscripts

b	borehole
e	extracting heat
f	fluid in tube
fd	fluid in down tube in a borehole
fu	fluid in up tube in a borehole
g	underground/thermal storage medium
i	number of the circuit
in	inlet temperature of GHE
out	outlet temperature of GHE
r	recharging heat
s	single borehole

Superscripts

$'$	fluid inlet temperature of a borehole or a circuit
$''$	fluid outlet temperature of a borehole or a circuit

Greek symbols

β	fraction of the heat transfer rate of each circuit
η	time ratio of heat injection and extraction
ρ	ground density (kg/m^3)
ε	thermal efficiency of a borehole
τ	time (s)

directly to the space heating system at temperatures between 40 °C and 70 °C.

It is well known that a large amount of industrial waste heat with high temperature, produced during the industrial processes, is usually squandered by way of cooling tower emissions into the atmosphere in the non-heating season. The seasonal thermal energy storage based on the vertical boreholes offers an efficient and favorable way to integrate the industrial waste heat with ground heat exchanger (GHE) which has serious cold accumulation. Using the GHE with vertical boreholes as a thermal storage region not only solves the storage problem of industrial waste heat in the non-heating season, but also mitigates the imbalance of the ground thermal load. As a result, the operation performance of GCHPs in heating mode can significantly improve.

The vertical boreholes of GCHP systems for conventional space heating and cooling are generally connected in parallel before being connected to the heat pump through the pipes, as shown in Fig. 1(a). Most industrial processes generally deliver industrial waste heat at a high temperature level of over 50 °C and require a cooling water at relatively lower return temperature, such as 20 °C. Obviously, the large temperature drop required by the industrial process cannot be realized through the conventional parallel connection of boreholes, which only achieve a temperature drop of 5 °C at most. In this study, a novel GHE configuration with multistage series is proposed to satisfy the high temperature gradient up to 15–20 °C, as shown in Fig. 1(b). The multistage series can not only effectively reduce the fluid temperature to a required low value, but also make full use of the industrial waste heat. Fig. 1 illustrates the two different borehole connection configurations, i.e. the parallel connection for GCHP systems and the multistage-series connection for the seasonal thermal storage of industrial waste heat.

The vertical GHE used for the seasonal thermal storage has the similar heat transfer mechanisms as conventional GHEs used for space heating and cooling. In the two cases, heat rejection/extraction into/from the ground is accomplished by the circulating fluid through U-shaped plastic pipes installed in boreholes. Since the 1980s, a number of models have been developed to evaluate GCHP systems using vertical boreholes for transferring heat to/from the ground based on analytical, numerical and hybrid models (Eskilson, 1987; Muraya et al., 1996; Kavanaugh, 1998; Hui and Spitler, 2002; Yang et al., 2009, 2010). Recently, a critical review and introduction to analytic models for vertical boreholes has been conducted in a perspective of time and space scales (Li and Lai, 2015).

However, most of existing models employed the conventional GHE configuration of in-parallel connection. Considering the high-grade thermal energy (70–90 °C) injected into the ground and the relatively large temperature drop through the GHE, it is necessary to design a complex configuration of the GHE mixed with parallel and series connections. Based on the available quantity of the industrial waste heat, a representative circuit with certain boreholes connected in parallel will be first designed and the number of the circuits connected in series will be determined according to the heat injection load and the required temperature drop. Little research is available to describe the heat transfer process of such a complex system. The main objectives of this paper are to develop a heat transfer model and design method of the multistage-series GHE for the seasonal thermal storage and to further investigate the thermal performance of the system.

2. Transient heat transfer model of vertical GHE with multistage-series circuits

2.1. Assumptions for the heat transfer model

As for a single borehole, the heat transfer process can be directly analyzed by means of the same mathematical methods as the conventional vertical borehole in GCHP systems. To keep the problem analytically manageable, the theoretical model of the multistage-series GHE is based on the following simplified assumptions:

(1) The ground is regarded as a homogeneous medium with a uniform initial temperature t_0, and its thermophysical properties do not change with temperature.
(2) The heat transfer in the ground is assumed to be carried out solely by heat conduction with the neglect of groundwater advection, using an effective ground thermal conductivity. The moisture migration in the ground is also negligible.
(3) Each circuit is composed of a number of boreholes connected in parallel with the same geometric parameters and thermal properties.
(4) The thermal interference between circuits is negligible because the heat transfer distance for most boreholes in each circuit is still within their own space region during the period of one recharging/extraction season.

2.2. Heat transfer model of multistage series GHE

For a given GHE configuration with multistage series, the main objective of the thermal analysis is to determine the optimal heat injection/extraction rate (Q_i) of each independent circuit and to

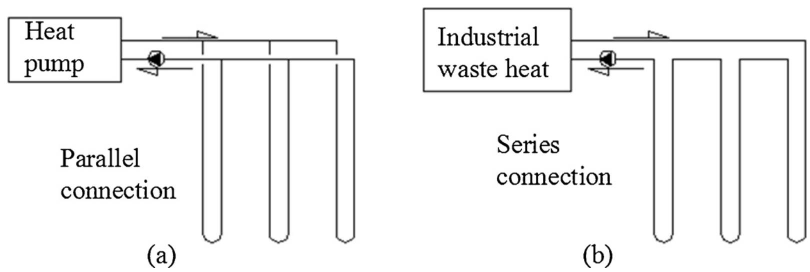

Fig. 1. (a) Conventional GHE in parallel connection. (b) Multistage-series GHE for the thermal storage based on the industrial waste heat.

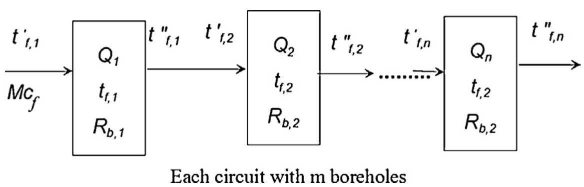

Fig. 2. The physical model of multistage series.

consequently obtain the inlet/outlet temperatures ($t_{f,i}'$, $t_{f,i}''$) of the circulating fluid of each circuit. In the following analysis, Q is the total heat transfer rate by the GHE and $\beta_i = Q_i/Q$ is defined as the heat transfer rate fraction which is a ratio of the heat transfer rate occupied by the ith circuit to the total heat transfer rate. Accordingly, the sum of all the β_i is equal to 1, i.e., $\sum_{i=1}^{n}\beta_i = 1$. Fig. 2 describes the physical model of the multistage series. Each circuit has a total of m boreholes connected in parallel with the assumption of the same heat transfer rate per unit length of each borehole (i.e., $q_{l,i} = Q_i/(mH)$). R_{bi} and $t_{f,i}$ are the borehole thermal resistance and the fluid average temperature of the ith circuit, respectively.

For each circuit, the heat injection rate to the surrounding ground by the ith circuit is equivalent to the heat rate transferred from the circulating fluid in the pipe to the borehole wall, based on the energy conservation law. The energy balance is given by the following equation:

$$\begin{cases} Q_i = Mc_f\left(t_{f,i}' - t_{f,i}''\right) \\ Q_i/mH = \left(\dfrac{t_{f,i}' + t_{f,i}''}{2} - t_{bi}\right)/R_{bi} \end{cases} \tag{1}$$

where t_{bi} is the representative borehole wall temperature of the ith circuit.

The inlet and outlet temperatures of the ith circuit can be easily derived according to Eq. (1):

$$\begin{cases} t_{f,i}' = t_{bi} + R_{bi}\beta_i Q/mH + \beta_i Q/(2Mc_f) \\ t_{f,i}'' = t_{bi} + R_{bi}\beta_i Q/mH - \beta_i Q/(2Mc_f) \end{cases} \tag{2}$$

The following two subsections presents the heat transfer models inside and outside the boreholes to achieve the borehole thermal resistance R_{bi} and the borehole wall temperature t_{bi} as well.

2.3. Thermal resistance inside the borehole

The quasi 3-D model of the heat transfer inside the borehole is employed to calculate the total borehole thermal resistance, which takes into account the 2-D heat conduction in the transverse cross-section as well as the convective heat transfer in the axial direction by the fluid inside the U-tubes. The energy equilibrium equations can be written for up-flow and down-flow of the circulating fluid:

$$\left.\begin{aligned} -M_s c_f \frac{dt_{f,u}}{dz} &= \frac{t_{f,u} - t_b}{R_1^{\Delta}} + \frac{t_{f,u} - t_{f,d}}{R_{12}^{\Delta}} \\ M_s c_f \frac{dt_{f,d}}{dz} &= \frac{t_{f,d} - t_b}{R_2^{\Delta}} + \frac{t_{f,d} - t_{f,u}}{R_{12}^{\Delta}} \end{aligned}\right\} \quad (0 \le z \le H) \tag{3}$$

Two conditions are necessary to complete the solution:

$$\left.\begin{aligned} z = 0, &\quad t_{f,u} = t_f' \\ z = H, &\quad t_{f,u} = t_{f,d} \end{aligned}\right\} \tag{4}$$

where $R_1^{\Delta} = (R_{11}R_{22} - R_{12}^2)/(R_{22} - R_{12})$, $R_2^{\Delta} = (R_{11}R_{22} - R_{12}^2)/(R_{11} - R_{12})$, $R_{12}^{\Delta} = (R_{11}R_{22} - R_{12}^2)/(R_{12})$. R_{11} and R_{22} are the thermal resistance between the circulating fluid and the borehole wall, and R_{12} is the resistance between the two pipes.

The general solution of this problem is derived by Laplace transformation, which is slightly complicated in form. At the instance of the symmetric placement of the U-tube inside the borehole, the temperature profiles in the two pipes were illustrated by Diao et al. (2004). For the purpose of practical applications an alternative parameter $\varepsilon = \left(t_f' - t_f'\right)/\left(t_f' - t_b\right)$ is derived from the temperature profiles, which is named as the heat transfer efficiency of the borehole. It should be noticed that t_f' and t_f'' are the entering/exiting fluid temperatures to/from the U-tube. From the derived temperature profile the more accurate heat conduction resistance between the fluid inside the U-tube and the borehole wall can be calculated by,

$$R_b = \frac{H}{M_s c_f}\left(\frac{1}{\varepsilon} - \frac{1}{2}\right) \tag{5}$$

2.4. Heat conduction outside the borehole

Based on the finite line source model, the temperature response on the borehole wall caused by its own heat flux, where $r = r_b$, was given by Zeng et al. (2002):

$$t_{b,s} = \frac{q_l}{4\pi\kappa_g}\int_0^H \left\{ \frac{erfc\left(\frac{\sqrt{r^2+(z-h)^2}}{2\sqrt{a\tau}}\right)}{\sqrt{r^2+(z-h)^2}} - \frac{erfc\left(\frac{\sqrt{r^2+(z+h)^2}}{2\sqrt{a\tau}}\right)}{\sqrt{r^2+(z+h)^2}} \right\} dh \quad + t_0 \tag{6}$$

where t_0 means the initial temperature of the ground. It is noticed that the borehole wall temperature varies with time and borehole depth. The temperature at the middle of the borehole depth ($z = 0.5H$) is usually chosen as its representative temperature.

Considering the thermal interference by the adjacent boreholes, the borehole wall temperature response, which is simultaneously caused by its heat flux and the surrounding boreholes, can be obtained through the superposition principle, as shown in Eq. (7):

$$t_b = t_{b,s}(r_b, 0.5H, \tau) + \sum_{i=1}^{m-1} t_{b,i}(r_i, 0.5H, \tau) \quad (7)$$

where m means the total number of the boreholes in a circuit and r_i is the distance between the representative borehole and the ith borehole.

2.5. Constraint conditions

The final aim of the thermal analysis for the GHE with n-stage series circuits is to seek the unique value of heat transfer rate ratio (i.e. β_i) and the inlet/outlet temperatures of each circuit for every time step with the constrain conditions. For the n-stage series, following the scheme shown in Fig. 2, the fluid outlet temperature of circuit 1 corresponds to the inlet temperature of circuit 2 and so on. Therefore, the coupled conditions are given as follows:

$$t'_{f,1} = t'_{f,2}, \ldots, t''_{f,i} = t'_{f,i+1}, \ldots, t''_{f,n-1} = t'_{f,n}$$

Accordingly, the objective function can be defined as:

$$\Delta = \left|\Delta_1\right| + \left|\Delta_2\right| + \cdots + \left|\Delta_{n-1}\right| \quad (8)$$

where $\Delta_1 = t''_{f,1} - t'_{f,2}$, $\Delta_i = t''_{f,i} - t'_{f,i+1}$ $(i = 1, \ldots, n-1)$ It is noticeable that the objective function is a function of the variables β_i (i = 1, 2, . . ., n), i.e. $\Delta = f(\beta_1, \beta_2, \ldots, \beta_n)$ according to Eq. (2). Theoretically, once the value of the objective function approaches to zero, the simulation model can determine the inlet/outlet temperatures of each circuit in the multistage series as well as the heat transfer rate fraction β_i.

2.6. The solution of the heat transfer model

In this study, the downhill simplex method is employed to search the optimal values of the heat transfer rate fractions, which is a local search method for optimization that can handle nonlinear problems. It is a closed geometric figure with N-dimensional straight line edges intersecting at $N+1$ vertices. In this method, three operations of reflection, expansion and contraction are employed to generate a new vertex point to substitute the worst point in the simplex. The first move is a reflection to generate a new vertex point and a new simplex which depend on the location of the worst point in the simplex. The new point is called the 'complement' of the worst point. The simplex procedures will be continued until they converge (Wang and Shoup, 2011).

The calculation program begins with an initial value of Q_1, for example an assumption of equal distribution of heat transfer rate, $\beta_1 = 1/n$ for the first time step. Then, the inlet/outlet temperatures of each circuit ($t'_{f,i}$ and $t''_{f,i}$) can be estimated using the thermal resistances inside and outside the borehole by Eqs. (2)–(7). The initial value of the objective function $\Delta = f(\beta_1, \beta_2, \ldots, \beta_n)$ will be derived for the first time step. Based on the downhill simplex method, an optimal minimum value of the objective function will be found, which satisfies the constraint conditions. Finally, the heat transfer rate and the inlet/outlet temperatures of each circuit can be obtained for the first time step. For the next time steps, the thermal resistances of the ground will be calculated based on the previous calculated heat rates and the current heat rate for each circuit. The same procedure can be employed to complete the whole operating time steps. Fig. 3 illustrates the detailed flowchart of the calculation process.

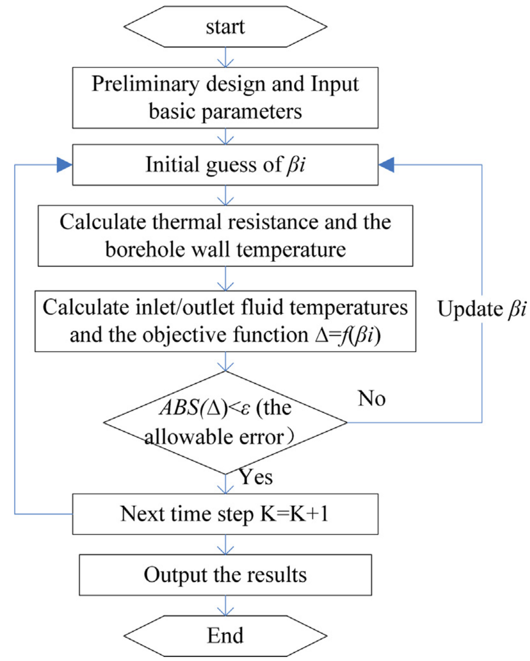

Fig. 3. Flowchart of the calculation process of the transient simulation model.

3. Steady flux heat transfer model of the seasonal thermal storage system

To design the required borehole size for an industrial seasonal thermal storage by means of the transient heat transfer model is actually a simulation-based process by means of the trial-and-error method to satisfy the user-specified minimum and maximum fluid temperatures. Meanwhile, the basic move that uses the downhill simplex method is also a complex and time-consuming process to find the optimum heat transfer rate and the inlet/outlet fluid temperatures of each circuit under the given conditions, such as the total injection/extraction heat loads, ground thermal properties and borehole configuration. Therefore, in this section, an empirical design method based on a steady flux heat transfer model is proposed to simplify the design process of the borehole size for the seasonal thermal storage system especially for the large capacity of boreholes (for example, over 1000 boreholes).

As for the transient heat transfer problem with adiabatic boundary conditions and a constant heat flux at the axis of the borehole, the temperature responses with time can be divided into two stages, one is the starting stage when the temperature is mainly affected by the distribution of the initial temperature and the other is the steady-flux stage. In the second stage, the temperature is independent of the space coordinate, but linearly increases with operating time.

For a seasonal thermal storage system with a large number of boreholes, the heat losses through the surrounding of the GHE region to the far field ground can be neglected because the thermal storage volume is significantly larger than the surface area of the GHE boundary. The heat transfer in the direction of the borehole axis, including the heat flux upwards through the ground surface and downwards into the deeper regions, can be neglected within a recharging or extracting period of a few months (Fang et al., 2002; Li et al., 2014). Therefore, the surface boundary of the individual region of each borehole can be assumed to be adiabatic. It is assumed that the recharging and extraction heat rates keep constant. Accordingly, it can be deduced that the temperature difference between the circulating fluid and the average temperature

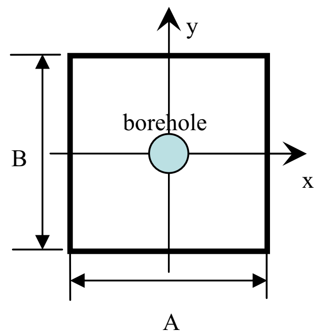

Fig. 4. Schematic diagram of borehole spacing.

of the thermal storage medium remains constant and is proportional to the heating rate q_l, as shown in the following equation:

$$t_g = \bar{t}_f - q_l \cdot R \tag{9}$$

where R means the total thermal resistance between the fluid in pipes and the thermal storage medium,

$$R = R_b + R_g \tag{10}$$

R_g is the steady flux thermal resistance between the borehole wall and the thermal storage medium. For a single borehole with a spacing of A in x direction and B in y direction, respectively, as shown in Fig. 4, the expression of the steady flux thermal resistance R_g can be calculated by the following equation (Hellstrom, 1991),(11)$R_g = \frac{1}{2\pi\kappa_g}\left[\ln\left(\frac{B}{2\pi r_b}\right) + \frac{\pi A}{6B}\right]$

It is obvious that the average temperatures of the circulating fluid and the surrounding ground will reach the highest value at the end of the heat injection season,

$$\bar{t}_{g,r} = \bar{t}_{f,r} - q_{l,r} \cdot R \tag{12}$$

where $q_{l,r}$ is the recharging heat flow rate per unit length of borehole.

Meanwhile, the average temperatures of the fluid and the surrounding ground will approach to the lowest value at the end of the heat extraction season,

$$\bar{t}_{g,e} = \bar{t}_{f,e} - q_{l,e} \cdot R \tag{13}$$

where $q_{l,e}$ is the extraction heat flow rate per unit length of borehole, which is negative in extracting heat season.

In order to keep the annual thermal balance of the underground, the annual accumulative recharging heat capacity is assumed equal to the amount of the annual extraction heat load. If the operating time ratio of the injection and extraction is given as $\eta = \tau_r/\tau_e$, the relation of the heat extraction rate and recharging heat rate is $q_{l,e} = -\eta q_{l,r}$ under the assumption of the constant heat flux during the whole recharging/extraction year.

During a heat injection season, the total recharging heat load of a single borehole can be expressed by the average temperature variation of the thermal storage medium surrounding the borehole (i.e. the thermal storage capacity of the surrounding ground),

$$q_{l,r}\tau_r = AB\rho_g c_g\left(\bar{t}_{g,r} - \bar{t}_{g,e}\right) \quad (\mathrm{J}) \tag{14}$$

According to Eqs. (12)–(14), the heat injection rate can be easily expressed by the peak temperature difference of the fluid between the recharging and extraction seasons.

$$q_{l,r} = \left(\bar{t}_{f,r} - \bar{t}_{f,e}\right) / \left[\frac{\tau_r}{AB\rho_g c_g} + R(\eta+1)\right] \tag{15}$$

For a given heat recharging load of $Q_S = q_{l,r}H$ and the maximum and minimum fluid temperatures of the recharging and extraction seasons, the total required borehole length can be roughly designed according to the following equation:

$$H = Q_s\left[\frac{\tau_r}{AB\rho_g c_g} + R(\eta+1)\right] / \left(\bar{t}_{f,r} - \bar{t}_{f,e}\right) \tag{16}$$

Table 1
Basic parameters of the case study.

Parameters	Values
The required average fluid temperature at the end of the injection season	65 °C (the inlet and outlet temperatures are 80 °C and 50 °C)
The required average fluid temperature at the end of the extraction season	22.5 °C (the inlet and outlet temperatures are 20 °C and 25 °C)
Ground thermal conductivity	1.9 W/(m K)
Ground density	1750 (kg/m^3)
Ground heat capacity	1000 (J/(kg K))

4. Case study

4.1. The preliminary design by steady flux heat transfer model

A copper industrial company located in Inner Mongolia China is taken as an example of the seasonal industrial heat storage of the GHE system. It is estimated that about 10 MW heat rate can be produced during the copper processing works. To keep the storage region heat balanced during a whole year, both the heat injection and extraction rates are set to 10 MW. The space heating time in Inner Mongolia is about 6 months, from October to next March. In order to make full use of the industrial waste heat from the copper works, the heat injection time is also scheduled to be 6 months which is from April to September.

It is necessary to give a preliminary design scheme before using the steady flux design method. In this case, the boreholes are buried in a matrix pattern with a spacing of 4 m and a depth of 100 m. The thermal properties of the surrounding ground (usually means the heat storage) are assumed to be uniform with an initial temperature of 12 °C. Each borehole with a radius of 75 mm consists of a single U-tube. The HDPE (PE 3408) pipes are adopted with an outer diameter of 32 mm and an inner diameter of 26 mm. The boundaries of the heat storage region are assumed to be heat adiabatic because of the large-scale boreholes. The other given parameters of the project are listed in Table 1.

Based on the aforementioned models, the borehole thermal resistance is calculated to be 0.2, and the total thermal resistance of the thermal storage medium is about 0.423. The required borehole length is calculated to be 329,814 m according to the simplified design method. Therefore, the designed GHE consists of 3300 boreholes with a depth of 100 m and is arranged in a matrix of 33 × 100 with a spacing of 4 m. The 3300 boreholes are divided into 3-stage series circuits each of which consists of 1100 boreholes connected in parallel configuration.

4.2. Comparison of the transient and steady flux heat transfer models

In order to validate the simplified steady-flux design method, the inlet and outlet temperatures of the circulating fluid can be simulated monthly by the transient heat transfer model under the design conditions obtained from the steady-flux method. It should be noticed that the steady flux solution does not take into account the initial transient process. Therefore, it is necessary to derive the transient time before the heat transfer process reaches the steady-flux state in the dynamic heat transfer model. According to the reference by Carslaw and Jaeger (1959), the transient time for the

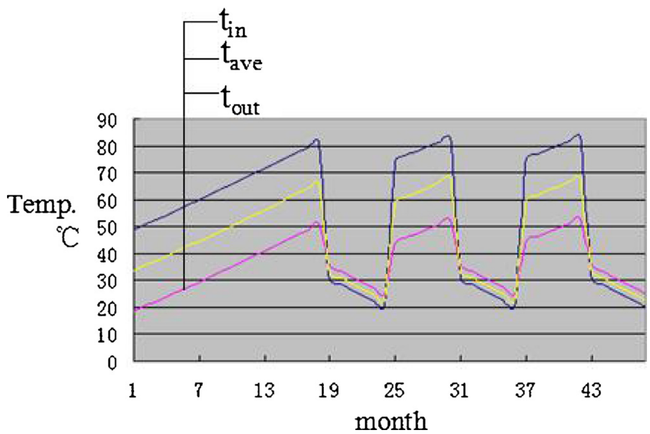

Fig. 5. Variations of the monthly simulated fluid temperatures of GHE with the 4 m spacing.

attenuation of the transient part can be estimated from solutions of the transient heat equation for an arbitrary initial temperature distribution in a rectangular area. For the quadratic borehole region, the initial time period to reach the steady-flux situation can be given by the following equation:

$$\frac{a\tau}{A^2} = \frac{3}{4\pi^2} \tag{17}$$

In this case study, the initial time period is estimated to be about 13 days for a borehole spacing of 4 m in sandy clay with $a = 1.08 \times 10^{-6}\,\mathrm{m^2/s}$. However, the annual injection/extraction seasons can periodically operate under the design conditions only when the temperatures of the circulating fluid and the heat storage could reach the prespecified values during the first heat injection season. According to the transient simulation results, it can be seen from Fig. 5 that the first heat injection period should be 18 months when the inlet temperature of the fluid reaches 80 °C. Fig. 5 also illustrates the variations of the inlet/outlet and the average temperatures of the fluid during the injection/extraction heat seasons. As shown in Fig. 5, the maximum inlet/outlet temperatures of the fluid at the end of the injection season are about 80 °C and 50 °C, respectively, while the minimum values at the end of the extraction season are about 20 °C and 25 °C. This indicates that the design solution from the steady flux method can basically satisfy the requirements of the injection and extraction heat process. The transient simulation results also demonstrate that the simplified steady-flux method can be applied to design a large-scale heat storage system.

5. Results and discussion

5.1. Discussion of the heat injection fractions of different circuits

It is noticed that the heat injection fraction of each circuit is different and varied with the operating time because the temperature difference between the average fluid and the local ground in each circuit region varies with time and gradually reduces along the flow direction. The difficult and key part of this heat transfer process is to accurately determine the time-dependent heat injection fraction of each circuit.

The transient heat transfer model incorporated with the downhill simplex method can be employed to solve the optimal value of the heat injection fraction of each circuit. The three-stage GHE with a total of 3300 single U-tube boreholes connected in series will be taken as an example to derive the heat injection ratios. For each circuit, 1100 boreholes are connected in parallel. Fig. 6 illustrates

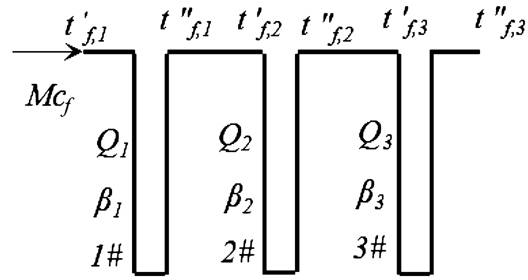

Fig. 6. The flowchart of the GHE with 3-stage series.

the schematic diagram of the three-stage series GHE. The objective function can be easily derived:

$$\begin{aligned}\Delta &= \left|t''_{f1} - t'_{f2}\right| + \left|t''_{f2} - t'_{f3}\right| \\ &= \left|\left(\beta_1 R_{b1} - \beta_2 R_{b2}\right) Q - \frac{\left(\beta_1 + \beta_2\right) Q}{2Mc_f} + t_{b1} - t_{b2}\right| \\ &\quad + \left|\left(\beta_2 R_{b2} - \beta_3 R_{b3}\right) Q - \frac{\left(\beta_2 + \beta_3\right) Q}{2Mc_f} + t_{b2} - t_{b3}\right|\end{aligned} \tag{18}$$

In order to illustrate the time-dependent effect of heat transfer rate of each circuit, the heat injection process is continually simulated for 24 months. The thermal resistances and borehole wall temperatures can be obtained according to the aforementioned transient model. The downhill simplex method is employed here to solve the mathematical problem of the three series circuits. Fig. 7 illustrates the variations of the heat rate fractions of three-stage series circuits against the simulation time. As Fig. 7 shows, the fraction of the first circuit is significantly higher than the second one and consequently the second one is higher than the third one because the temperature gradient between the former circuit and the surrounding ground is higher compared to the latter circuit. The highest fraction of the first circuit reaches 0.58 at the beginning of the operation. It is noticed that the sum of the fractions of the three circuits equals one.

5.2. Effect of borehole spacing on the thermal performance

It is obvious that a smaller spacing between boreholes leads to a smaller thermal storage volume and a significant thermal

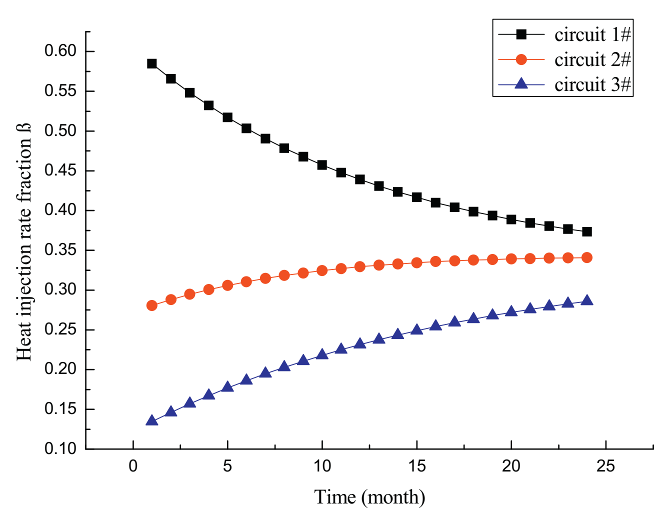

Fig. 7. Injection heat rate fractions with simulation time.

Table 2
Thermal properties of different soils.

Soil type	Density (kg/m^3)	Heat capacity (J/(kg K))	Thermal conductivity (W/(m K))	Thermal diffusivity $\times 10^6$ m^2/s
Clay	1285	1200	0.8	0.519
Sandy clay	1750	1000	1.9	1.08
Siltstone	2570	1556	3.2	0.8

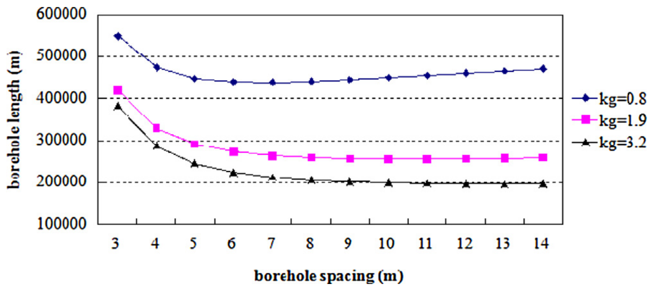

Fig. 8. The variations of designed borehole length with spacing.

interference between boreholes reducing the thermal performance of the heat injection/extraction process. However, too large spacing means a large volume of thermal storage which may be difficult to enhance the ground temperature to required value during the heat storage season and consequently difficult to provide enough heating load required by the space heating system under the same heat injection quantity as the case with smaller spacing. Therefore, there is an optimal borehole spacing for the seasonal heat storage. Fig. 8 describes the variations of the required borehole length with the spacing under different conditions of ground thermal conductivity. It can be seen from Fig. 8 that the designed borehole length is significantly reduced with the increase of the spacing under the conditions of small spacing and then becomes slightly larger with the increase of the spacing after reaching a lowest value at some point.

This indicates a slight difference from the conventional GHE only for space heating and cooling. For the conventional GHE, the larger spacing usually means a better thermal performance consequently causing a shorter borehole length. However, for the GHE with thermal storage, there is an optimal borehole spacing. Actually, the optimal borehole spacing from the view point of the annual heat injection and extraction can be easily obtained by calculating the derivative of spacing in Eq. (16) in the case of quadratic spacing. The details of the derivation can be found in Appendix A.

$$A = \sqrt{\frac{4\pi k_g \tau_r}{\rho_g c_g(\eta + 1)}} \tag{19}$$

It should be noticed that the larger spacing will increase the capital cost for a vast amount of land. Therefore, it is necessary to determine a reasonable borehole spacing by a comprehensive economic analysis of costs of drilling and land and the thermal performance of the system.

5.3. *Effect of ground thermal properties on the thermal performance*

The ground thermal properties are the critical factors which can thermally influence to a large extent the storage performance of the GHE. In this study, three types of soils (clay, sandy clay and siltstone) are selected as heat storage mediums for comparisons of their individual heat transfer capability. The thermal properties of these soils are listed in Table 2.

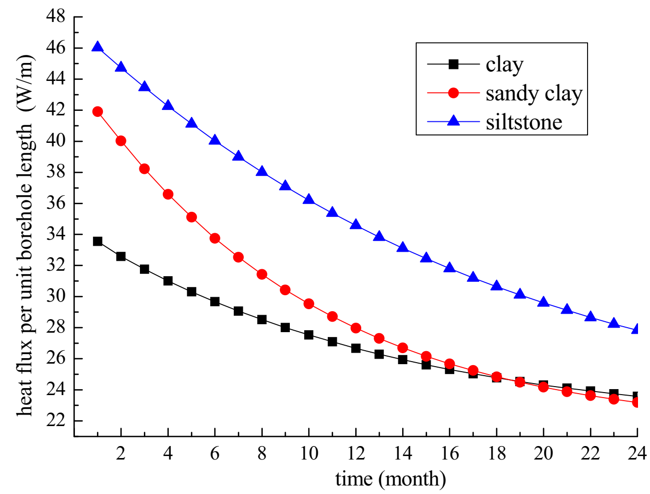

Fig. 9. Effect of the soil thermal properties on heat injection rate per unit borehole length.

Fig. 9 shows the sensitivity of the heat injection rate per unit length of borehole to the soil thermal properties for the three cases of soils during the 2 years of continuous heat injection. Evidently, all the heat transfer rates of the three kinds of soils are decreased with time due to the gradually reduced temperature gradient between the fluid and the ground. The siltstone behaves the highest heat flux because of its largest thermal conductivity and heat capacity. The heat transfer rate of the sandy clay is larger at the beginning of the heat injection period because of its larger thermal conductivity and becomes lower compared to the clay at the end of the simulation. This is due to the lower heat capacity of the sandy clay, which results in a higher temperature rise among the surrounding soil and consequently a performance degradation. Therefore, the recharging heat performance of the GHE in the ground is comprehensively influenced by the thermal conductivity and heat capacity of the ground. It can be seen from Fig. 8 that the thermal conductivity of the ground plays an important role in determining the thermal performance of the heat storage system.

6. Conclusions

A novel borehole configuration of multistage-series circuits is proposed for the seasonal thermal storage based on industrial waste heat. A transient simulation model of multistage-series circuits is developed to illustrate the heat transfer process of the underground thermal storage. The simplex method is employed to solve the fluid temperature and the heat transfer rate of each circuit. Meanwhile, a steady flux heat transfer model which can be applied to easily design the underground thermal storage system with large-scale boreholes is also established in this paper. The heat injection rate fractions of the multistage circuits are calculated in a case of three-stage thermal storage system. A set of parameters that strongly affect the thermal performance of the GHE with multistage series circuits is discussed in detail. The main conclusions obtained from this study are listed as follows:

(1) The heat injection rate ratio of the first circuit is the largest among all the circuits due to the largest temperature gradient between the borehole and the surrounding soil. It is noteworthy that the ground temperature rise or decrease nearby the former circuits is significant compared to the ground temperature changes nearby the latter circuits. As a result, the heat transfer efficiency of the former circuits reduces considerably.
(2) In order to equilibrate the ground temperature for multistage circuits, it is recommended to reverse the flow direction at regular time intervals to enhance the total heat transfer efficiency of the GHE system.
(3) The influence of the borehole spacing on thermal performance is considerable, especially for closer borehole spacing. Generally, there is an optimal borehole spacing which results in a smallest borehole size.
(4) The ground thermal properties also play an important role in determining the GHE size and the thermal efficiency of the system. Therefore, it is necessary for designers and engineers to obtain dependable on-site data of the thermal properties of the ground as a basis for designing an optimum seasonal thermal storage system.

Acknowledgment

The work has been supported by a grant from National Natural Science Foundation of China (Project No. 51208286) and a grant from 12th Five-Year National Science and Technology Support Program (2012BAJ06B03).

Appendix A. Derivation of the borehole spacing *A*

In the following calculation, the borehole spacing is set to equal, i.e. $A = B$. It can be deduced from the following equation that the designed borehole length is a function of the variable of the borehole spacing for a specific case with given recharging/extraction heat rate and time,

$$H = Q_s \left[\frac{\tau_r}{AB\rho_g c_g} + R(\eta + 1) \right] / \left(\bar{t}_{f,r} - \bar{t}_{f,e} \right) \quad \text{(A1)}$$

where $R = R_b + \frac{1}{2\pi\kappa_g} \left[\ln \left(\frac{B}{2\pi r_b} \right) + \frac{\pi A}{6B} \right]$

The minimal value of borehole depth (H) can be obtained by calculating the derivative of A and then setting $dH/dA = 0$,

$$\frac{d\left(Q_s \left[\frac{\tau_r}{A^2\rho_g c_g} + \left(R_b + \frac{1}{2\pi\kappa_g} \left[\ln\left(\frac{A}{2\pi r_b} \right) + \frac{\pi A}{6A} \right] \right) (\eta + 1) \right] / \left(\bar{t}_{f,r} - \bar{t}_{f,e} \right) \right)}{dA} = 0 \quad \text{(A2)}$$

Therefore, the optimal borehole spacing corresponding to the minimum borehole length can be obtained through Eq. (A2),

$$A = \sqrt{\frac{4\pi k_g \tau_r}{\rho_g c_g (\eta + 1)}} \quad \text{(A3)}$$

References

Bayer, P., De Paly, M., Beck, M., 2014. Strategic optimization of borehole heat exchanger field for seasonal geothermal heating and cooling. Appl. Energy 136, 445–453.
Carslaw, H.S., Jaeger, J.C., 1959. Conduction of Heat in Solids, 2nd edition. Oxford University Press, New York, USA.
Chen, X., Yang, H.X., Lu, L., Wang, J.G., Liu, W., 2011. Experimental studies on a ground coupled heat pump with solar thermal collectors for space heating. Energy 36 (8), 5292–5300.
Diao, N.R., Zeng, H.Y., Fang, Z.H., 2004. Improvement on modelling of heat transfer in vertical ground heat exchangers. Int. J. HVAC&R Res. 10 (4), 459–470.
Eskilson, P., 1987. Thermal Analysis of Heat Extraction Boreholes. University of Lund, Sweden (Ph.D. thesis).
Farzin, M.R., Fung, A.S., Leong, W.H., 2013. Feasibility of combined solar thermal and ground source heat pump systems in cold climate. Energy Build. 61, 224–232.
Fang, Z.H., Diao, N.R., Cui, P., 2002. Discontinuous operation of geothermal heat exchangers. Tsinghua Sci. Technol. 7 (2), 194–197.
Hellstrom, G., 1991. Ground Heat Storage, Thermal Analysis of Duct Storage Systems. Department of Mathematical Physics, University of Lund, Sweden (Doctoral thesis).
Hui, J., Spitler, J.D., 2002. A parameter estimation based model of water-to-water heat pumps for use in energy calculation programs. ASHRAE Trans. 108 (1), 3–17.
Kavanaugh, S.P., 1998. A design method for hybrid ground-source heat pumps. ASHRAE Trans. 104 (2), 691–698.
Kjellsson, E., Hellstrom, G., Perers, B., 2010. Optimization of systems with the combination of ground-source heat pump and solar collectors in dwellings. Energy 35 (6), 2667–2673.
Li, M., Lai, A.C.K., 2015. Review of analytical models for heat transfer by vertical ground heat exchangers (GHEs): a perspective of time and space scales. Appl. Energy 151, 178–191.
Li, M., Li, P., Chan, V., Lai, A.C.K., 2014. Full-scale temperature response function (G-function) for heat transfer by borehole ground heat exchangers (GHEs) from sub-hour to decades. Appl. Energy 136, 197–205.
Muraya, N.K., O'Neal, D.L., Heffington, W.M., 1996. Thermal interference of adjacent legs in a vertical U-tube heat exchanger for a ground-coupled heat pump. ASHRAE Trans. 102 (2), 12–21.
Ozgener, O., Hepbasli, A., 2007. A parametrical study on the energetic and exergetic assessment of a solar-assisted vertical ground-source heat pump system used for heating a greenhouse. Build. Environ. 42 (14), 11–24.
Pinel, P., Cruickshank, C.A., Beausoleil-Morrison, L., Wills, A., 2011. A review of available methods for seasonal storage of solar thermal energy in residential applications. Renew. Sust. Energy Rev. 15 (7), 3341–3359.
Reuss, M., Beck, M., Müller, J.P., 1997. Design of a seasonal thermal energy storage in the ground. Solar E 59, 247–257.
Self, S.J., Reddy, B.V., Rosen, M.A., 2013. Geothermal heat pump systems: status review and comparison with other heating options. Appl. Energy 101, 341–348.
Si, Q., Okumiya, M., Zhang, X.S., 2014. Performance evaluation and optimization of a novel solar-ground source heat pump system. Energy Build. 70, 237–245.
Spitler, J.D., 2005. Ground-source heat pump system research—past, present, and future. HVAC&R Res. 11, 165–167.
Trillat-Berdal, V., Souyri, B., Fraisse, G., 2006. Experimental study of a ground-coupled heat pump combined with thermal solar collectors. Energy Build. 38 (12), 1477–1484.
Wang, P.C., Shoup, T.E., 2011. Parameter sensitivity study of the Nelder–Mead Simplex Method. Adv. Eng. Softw. 42 (7), 529–533.
Yang, H.X., Cui, P., Fang, Z.H., 2010. Vertical-borehole ground-coupled heat pumps: a review of models and systems. Appl. Energy 87, 16–27.
Yang, W.B., Shi, M.H., Dong, H., 2006. Numerical simulation of the performance of a solar-earth source heat pump system. Appl. Therm. Eng. 26, 2367–2376.
Yang, W.B., Shi, M.H., Liu, G.Y., Chen, Z.Q., 2009. A two-region simulation model of vertical U-tube ground heat exchanger and its experimental verification. Appl. Energy 86 (10), 2005–2012.
Zeng, H.Y., Diao, N.R., Fang, Z.H., 2002. A finite line-source model for boreholes in geothermal heat exchangers. Heat Transf. Asian Res. 31 (7), 558–567.
Zhu, N., Hu, P.F., Xu, L.H., Jiang, Z.N., Lei, F., 2014. Recent research and applications of ground source heat pump integrated with thermal energy storage systems: a review. Appl. Therm. Eng. 71 (1), 142–151.